

Section S1

Linearization of transfer function for sedimentary denitrification

This section expands on the transformations applied to the non-linear transfer function for sedimentary denitrification presented by Bohlen et al. (2012) in order to use the transfer function in our linear N cycle model. The original function is as follows:

1. $\text{DIN loss} = (0.60 + 0.19 \cdot 0.99^{(\text{O}_2 - \text{NO}_3^-)_{\text{bottom}}}) \cdot \text{RRPOC}$ for water depths $\geq 1000\text{m}$
2. $\text{DIN loss} = 0.73 \cdot (0.60 + 0.19 \cdot 0.99^{(\text{O}_2 - \text{NO}_3^-)_{\text{bottom}}}) \cdot \text{RRPOC}$ for water depths $< 1000\text{m}$

The calculation of the rain rate of particulate organic carbon (RRPOC) follows the Martin curve is as described in Text S4 (Equation 20). $(\text{O}_2 - \text{NO}_3^-)_{\text{bottom}}$ is the difference between $[\text{O}_2]$ and $[\text{NO}_3^-]$ at the bottom of the water column, where it interfaces with the sediments.

For every model grid box, the depth is taken to be the depth at the bottom of the box. Each box is then assigned a multiplier of 1 (if depth $\geq 1000\text{m}$) or 0.73 (if depth $< 1000\text{m}$) that will be multiplied by the sedimentary denitrification terms.

The next step is linearizing the (DIN loss)/RRPOC data presented by Bohlen et al. (2012) with respect to $(\text{O}_2 - \text{NO}_3^-)_{\text{bottom}}$, since we cannot use the exponential equation in our linear system. This was performed by selecting two $(\text{O}_2 - \text{NO}_3^-)_{\text{bottom}}$ cutoff points (29 μM and 141 μM), breaking the data into three groups. A piecewise linear regression was then performed on each of these sections (Figure S1), resulting in the following equations:

3. $(\text{DIN loss})/\text{RRPOC} = 0.297 - 0.005(\text{O}_2 - \text{NO}_3^-)_{\text{bottom}}$ $(\text{O}_2 - \text{NO}_3^-)_{\text{bottom}} \leq 29 \mu\text{M}$
4. $(\text{DIN loss})/\text{RRPOC} = 0.222 - 0.001(\text{O}_2 - \text{NO}_3^-)_{\text{bottom}}$ $29 \mu\text{M} < (\text{O}_2 - \text{NO}_3^-)_{\text{bottom}} \leq 141 \mu\text{M}$
5. $(\text{DIN loss})/\text{RRPOC} = 0.105 - 0.000006(\text{O}_2 - \text{NO}_3^-)_{\text{bottom}}$ $141 \mu\text{M} < (\text{O}_2 - \text{NO}_3^-)_{\text{bottom}}$

These $(\text{O}_2 - \text{NO}_3^-)_{\text{bottom}}$ cutoff points were then converted to O_2 cutoff points in order to use a simple N-independent mask to determine which of the relationships to apply to a given model grid box. A linear relationship between $[\text{O}_2]$ and $(\text{O}_2 - \text{NO}_3^-)_{\text{bottom}}$ was determined using The 2013 World Ocean Atlas interpolated data product for $[\text{O}_2]$ and $[\text{NO}_3^-]$ (Garcia et al., 2014). The linear relationship is as follows and is also shown in Figure S2:

$$6. (O_2-NO_3^-)_{\text{bottom}} = 1.12[O_2]_{\text{bottom}} - 55.6$$

The $(O_2-NO_3^-)_{\text{bottom}}$ cutoff points can then be expressed in $[O_2]$ units as 75 and 175 μM .

The final step in modifying this transfer function for use in the linear model is to break the piecewise linear equations into a component that is dependent on N and a component that is independent of N. This facilitates the implementation of the equations in our linear system.

$$7. \text{Independent} + \text{dependent} = (\text{DIN loss})/\text{RRPOC}$$

$$8. \text{Independent} = 0.297 - 0.005[O_2] \quad O_2 \leq 75 \mu\text{M}$$

$$9. \text{Dependent} = 0.005[NO_3^-]$$

$$10. \text{Independent} = 0.222 - 0.001[O_2] \quad 75 \mu\text{M} < O_2 \leq 175 \mu\text{M}$$

$$11. \text{Dependent} = 0.001[NO_3^-]$$

$$12. \text{Independent} = 0.105 - 0.000006[O_2] \quad 175 \mu\text{M} < O_2$$

$$13. \text{Dependent} = 0.000006[NO_3^-]$$

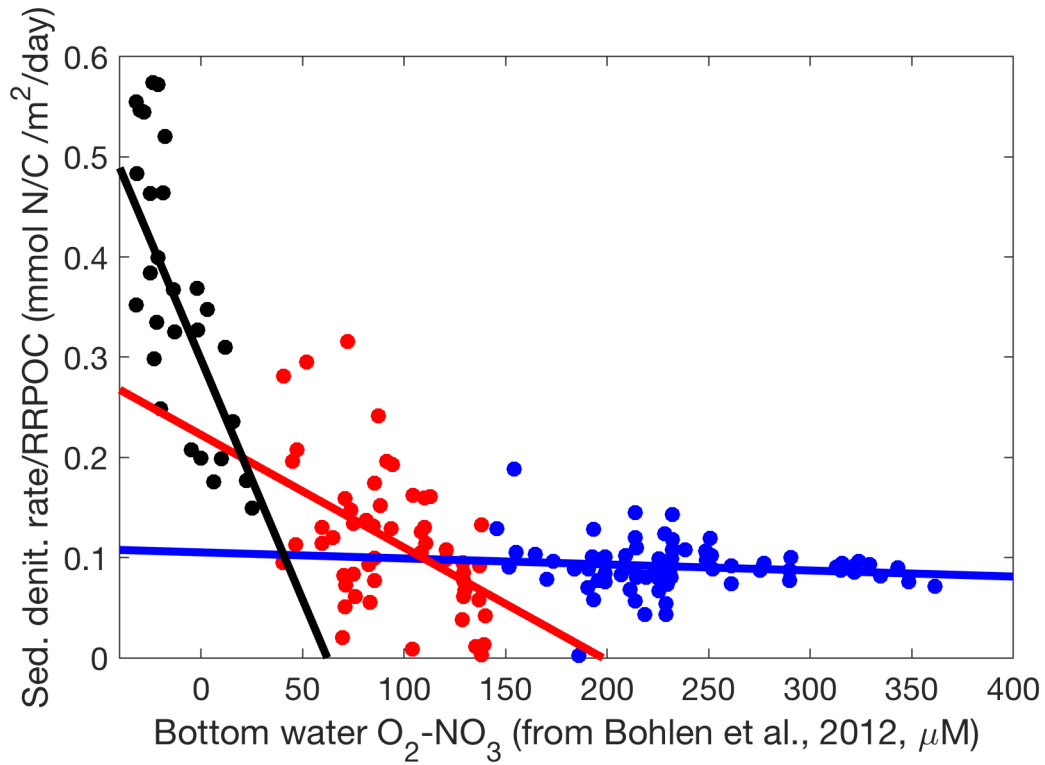


Figure S1. Piecewise division of the transfer function for sedimentary denitrification from Bohlen et al. (2012). In order to incorporate this into our liner model, we split the original non-linear relationship between sedimentary denitrification rate, rain rate of particulate organic carbon (RRPOC), and bottom water ($[O_2] - [NO_3^-]$) into three linear segments with cutoff points in terms of ($[O_2] - [NO_3^-]$). These cutoff points were then converted to $[O_2]$ cutoff points using a relation shown in Figure S2.

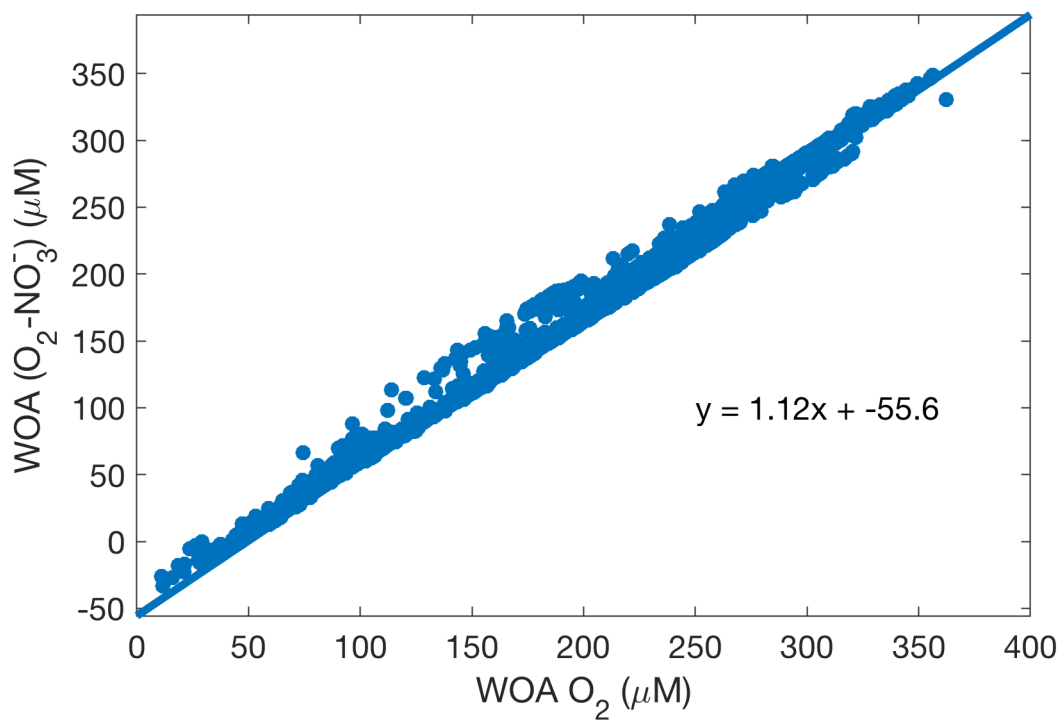


Figure S2. Plot of 2013 World Ocean Atlas [O₂] vs. ([O₂] - [NO₃⁻]) (Garcia et al., 2014). In order to express the sedimentary denitrification transfer function cutoff points (Figure S1) in terms of [O₂] rather than ([O₂] - [NO₃⁻]), we determined a linear relationship between [O₂] and ([O₂] - [NO₃⁻]).

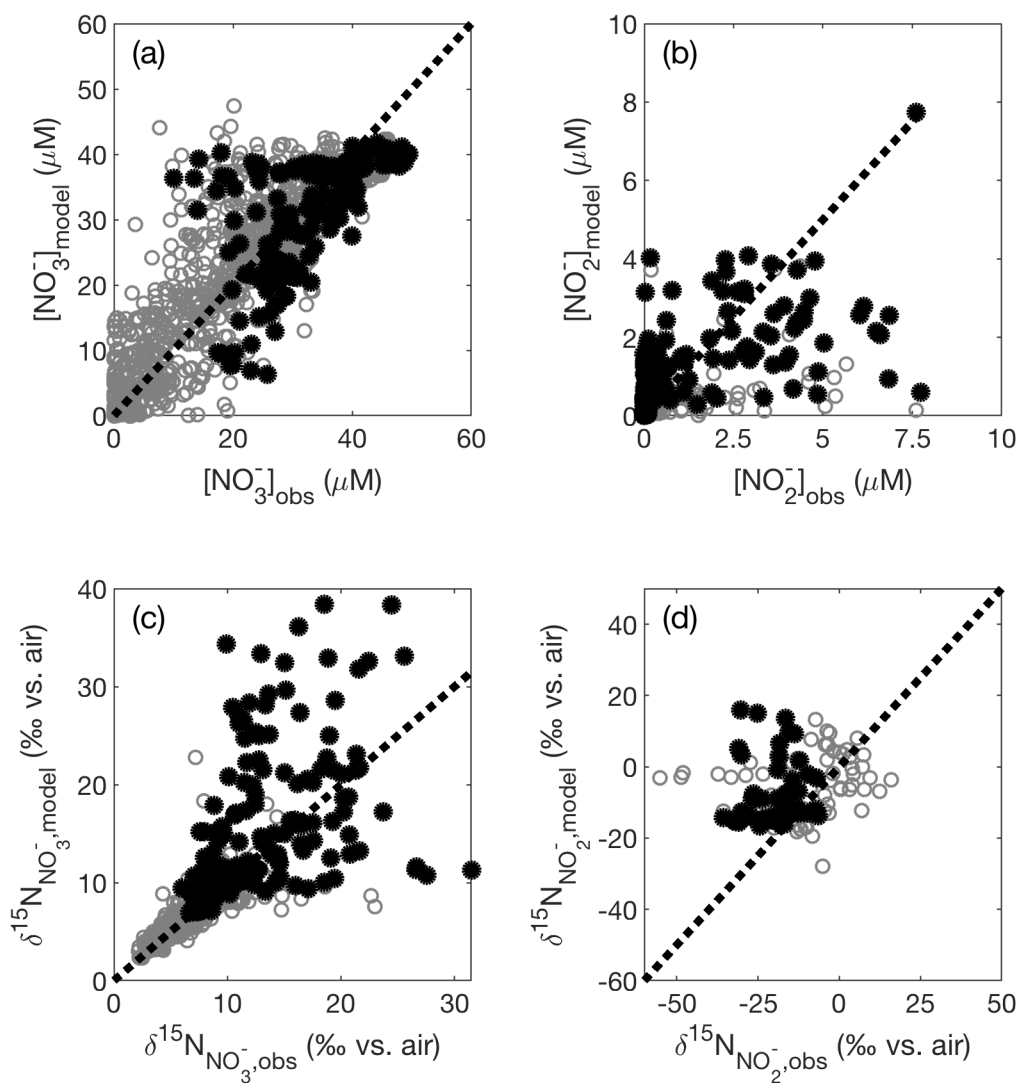


Figure S3. Modeled (a) $[\text{NO}_3^-]$, (b) $[\text{NO}_2^-]$, (c) $\delta^{15}\text{N}_{\text{NO}_3^-}$, and (d) $\delta^{15}\text{N}_{\text{NO}_2^-}$ are compared against the corresponding values from the database training set. Shown on each panel is a 1:1 line starting at the origin. Data in black have corresponding $[O_2] < 10 \mu\text{M}$, and data in gray have $[O_2] \geq 10 \mu\text{M}$.

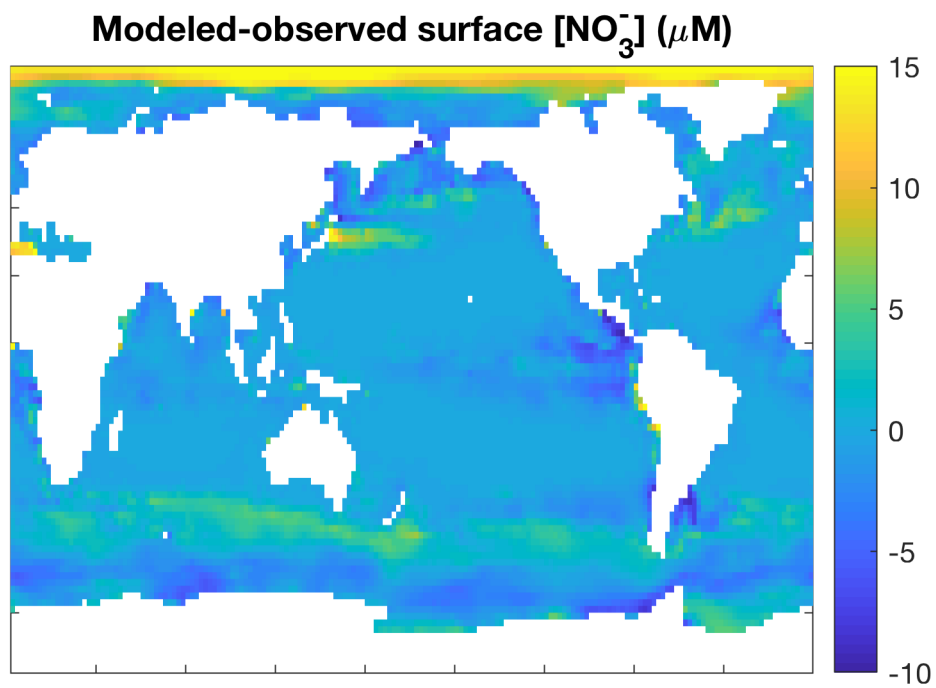


Figure S4. Map showing a comparison between modeled surface $[\text{NO}_3^-]$ for the top two model boxes and 2013 WOA $[\text{NO}_3^-]$ (Garcia et al., 2014) interpolated to the model grid for the same depths. Areas where the model overpredicts surface $[\text{NO}_3^-]$ are shown in yellow, and underprediction is shown in blue.

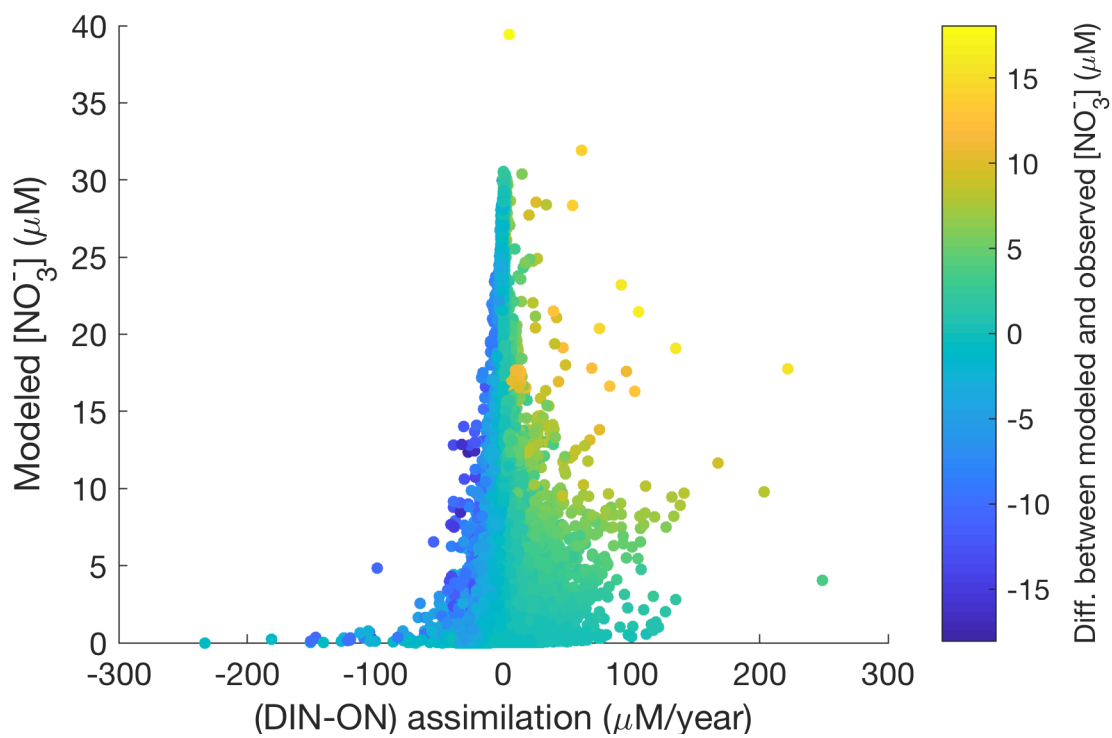


Figure S5. Difference in assimilation rates between the DIN and ON model runs plotted against the modeled $[\text{NO}_3^-]$. Points are colored by the difference between modeled and observed $[\text{NO}_3^-]$.

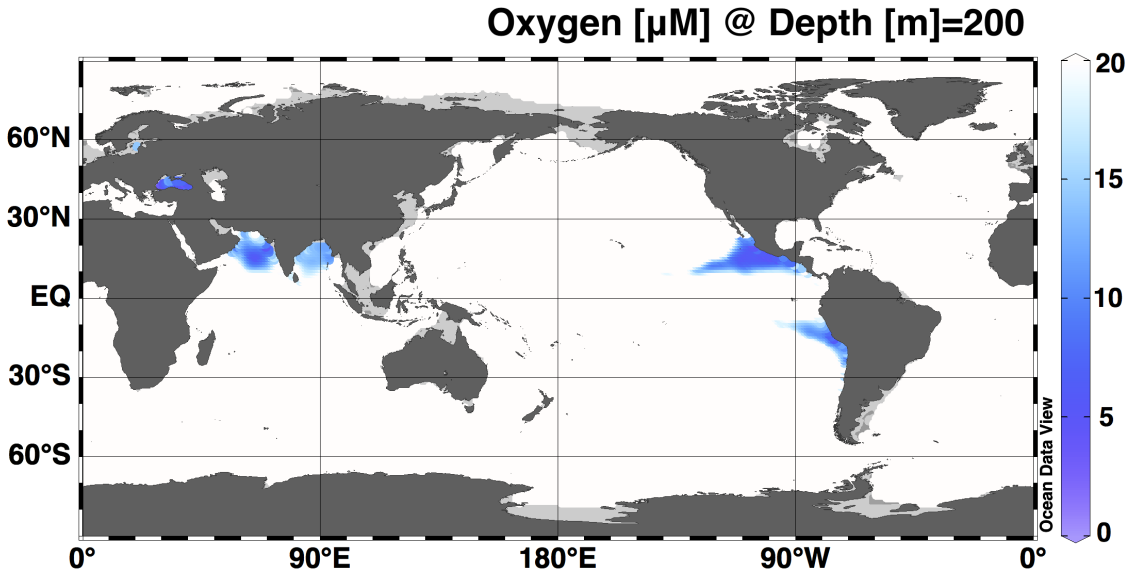


Figure S6. Map of annual average 2013 World Ocean Atlas [O_2] @ 200m depth (Garcia et al., 2014) to demonstrate areas where O_2 is low enough for anoxic processes such as nitrate reduction, nitrite reduction, and anammox. The canonical ODZs are visible in blue: the Arabian Sea, ETNP, and ETSP. Also shown in blue are the Bay of Bengal and the Black Sea.

Location and year sampled	Data types	Reference
ETNP, 2003	[NO ₃ ⁻], [NO ₂ ⁻], δ ¹⁵ N _{NO3-} , δ ¹⁵ N _{NO2-}	Casciotti and McIlvin, 2007
ETNP, 2012	[NO ₃ ⁻], [NO ₂ ⁻], δ ¹⁵ N _{NO3-} , δ ¹⁵ N _{NO2-}	Casciotti, unpublished
ETSP, 2011	[NO ₃ ⁻], [NO ₂ ⁻], δ ¹⁵ N _{NO3-} , δ ¹⁵ N _{NO2-}	Casciotti, unpublished
ETSP, 2013	[NO ₃ ⁻], [NO ₂ ⁻], δ ¹⁵ N _{NO3-} , δ ¹⁵ N _{NO2-}	Peters et al., 2018

Table S1. New additions to the database originally compiled by Rafter et al. (in prep.).

References

1. Bohlen L, Dale AW, Wallmann K. Simple transfer functions for calculating benthic fixed nitrogen losses and C:N:P regeneration ratios in global biogeochemical models. *Global Biogeochem Cycles*. 2012;26(3). doi:10.1029/2011GB004198.
2. Casciotti KL, McIlvin MR. Isotopic analyses of nitrate and nitrite from reference mixtures and application to Eastern Tropical North Pacific waters. *Mar Chem*. 2007;107(2):184-201. doi:10.1016/j.marchem.2007.06.021.
3. Garcia HE, Boyer TP, Locarnini RA, et al. World Ocean Atlas 2013. Volume 3: Dissolved oxygen, apparent oxygen utilization, and oxygen saturation. NOAA Atlas NESDIS 75, 27 pp. 2013.
4. Garcia HE, Locarnini RA, Boyer TP, et al. World Ocean Atlas 2013, Volume 4: Dissolved inorganic nutrients (phosphate, nitrate, silicate). NOAA Atlas NESDIS 76, 25 pp. 2013.
5. Peters BD, Lam PJ, Casciotti KL. Nitrogen and oxygen isotope measurements of nitrate along the US GEOTRACES Eastern Pacific Zonal Transect (GP16) yield insights into nitrate supply, remineralization, and water mass transport. *Mar Chem*. 2018;201:137-150. doi:10.1016/j.marchem.2017.09.009.